

Characterization of the Inhibitor Binding Site in Mitochondrial NADH–Ubiquinone Oxidoreductase by Photoaffinity Labeling Using a Quinazoline-Type Inhibitor[†]

Masatoshi Murai,[‡] Koji Sekiguchi,[‡] Takaaki Nishioka,[§] and Hideto Miyoshi*

Division of Applied Life Sciences, Graduate School of Agriculture, Kyoto University, Sakyo-ku, Kyoto 606-8502, Japan

Received October 27, 2008; Revised Manuscript Received December 5, 2008

ABSTRACT: The diverse inhibitors of bovine heart mitochondrial complex I (NADH–ubiquinone oxidoreductase) are believed to share a common large binding domain with partially overlapping sites, though it remains unclear how these binding sites relate to each other. To obtain new insight into the inhibitor binding domain in complex I, we synthesized a photoreactive azidoquinazoline {[¹²⁵I]-6-azido-4-(4-iodophenethylamino)quinazoline, [¹²⁵I]AzQ}, in which a photolabile azido group was introduced into the toxophoric quinazoline ring to allow specific cross-linking, and carried out a photoaffinity labeling study using bovine heart submitochondrial particles. Analysis of the photo-cross-linked proteins by peptide mass fingerprinting and immunoblotting revealed that [¹²⁵I]AzQ specifically binds to the 49 kDa and ND1 subunits with a frequency of ~4:1. The cross-linking was completely blocked by excess amounts of other inhibitors such as acetogenin and fenpyroximate. Considerable cross-linking was also detected in the ADP/ATP carrier and 3-hydroxybutyrate dehydrogenase, though it was not associated with dysfunction of the two proteins. The partial proteolysis of the [¹²⁵I]AzQ-labeled 49 kDa subunit by V8-protease and N-terminal sequencing of the resulting peptides revealed that the amino acid residue cross-linked by [¹²⁵I]AzQ is within the sequence region Thr25–Glu143 (118 amino acids). Furthermore, examination of fragment patterns generated by exhaustive digestion of the [¹²⁵I]AzQ-labeled 49 kDa subunit by V8-protease, lysylendopeptidase, or trypsin strongly suggested that the cross-linked residue is located within the region Asp41–Arg63 (23 amino acids). The present study has revealed, for the first time, the inhibitor binding site in complex I at the sub-subunit level.

The proton-pumping NADH–ubiquinone oxidoreductase (complex I)¹ is the first energy-transducing enzyme of the respiratory chains of most mitochondria and many bacteria. It catalyzes the oxidation of NADH by ubiquinone, coupled to the generation of an electrochemical proton gradient across the membrane that drives energy-consuming processes such as ATP synthesis and flagella movement (1). Complex I is the most complicated multisubunit enzyme in the respiratory chain; e.g., the enzyme from bovine heart mitochondria is composed of 45 different subunits with a total molecular mass of about 1 MDa (2). Recently, the crystal structure of

the hydrophilic domain (peripheral arm) of complex I from *Thermus thermophilus* was solved at 3.3 Å resolution, revealing the subunit arrangement and the putative electron transfer pathway (3). However, our knowledge about the functional and structural features of the membrane arm, such as the ubiquinone redox reaction, proton translocation mechanism, and mode of action of numerous specific inhibitors, is still highly limited (4–7).

A variety of inhibitors act at the terminal electron transfer step of bovine complex I (8–10). Although these inhibitors are generally believed to act at the ubiquinone reduction site (11), there is still no strong experimental evidence to verify this (12, 13). Radio-ligand and fluorescent-ligand binding studies (14, 15) suggested that the chemically diverse inhibitors share a common large binding domain with partially overlapping sites in bovine complex I, though it remains unclear how the binding sites of the inhibitors relate to each other. Mutagenesis studies using the yeast *Yarrowia lipolytica* and *Rhodobacter capsulatus* (16–19) and photo-affinity labeling studies (20–23) have indicated that the PSST, 49 kDa, ND1, and ND5 subunits contribute to the inhibitor binding domain. On the other hand, taking into consideration the unique inhibitor Δlac-acetogenins whose site of action entirely differs from that of traditional inhibitors (23–25), one cannot exclude the possibility that there are further diverse chemicals that disturb the function of the membrane domain differently depending on their structural specificity.

[†] This work was supported in part by a Grant-in-Aid for Scientific Research from the Japan Society for the Promotion of Science (Grant 20380068 to H.M.) and a Grant-in-Aid for JSPS Fellows (to M.M.).

* Corresponding author: e-mail, miyoshi@kais.kyoto-u.ac.jp; tel, +81-75-753-6119; fax, +81-75-753-6408.

[‡] These authors contributed equally to the manuscript.

[§] Present address: Institute for Advanced Biosciences, Keio University, Tsuruoka 997-0035, Japan.

¹ Abbreviations: AQ, 6-amino-4-(4-*tert*-butylphenethylamino)quinazoline; AzQ, 6-azido-4-(4-iodophenethylamino)quinazoline; [¹²⁵I]AzQ, ¹²⁵I-labeled AzQ; BN-PAGE, blue-native polyacrylamide gel electrophoresis; CBB, Coomassie brilliant blue; complex I, mitochondrial proton-pumping NADH–ubiquinone oxidoreductase; DDM, *n*-dodecyl β-D-maltoside; DTT, dithiothreitol; IC₅₀, the molar concentration (nM) needed to reduce the control NADH oxidase activity in SMP by half; IEF, isoelectric focusing; IPG, immobilized pH gradient; MALDI-TOF, matrix-assisted laser desorption ionization time of flight; MS, mass spectrometry; PVDF, polyvinylidene fluoride; SDS–PAGE, sodium dodecyl sulfate–polyacrylamide gel electrophoresis; SMP, submitochondrial particles.

The photoaffinity labeling technique is a powerful means of studying the interaction of biologically significant chemicals with their target macromolecules (26, 27). The method allows for the identification of the target and also the binding domain within the target protein. In general, a photoaffinity probe is synthesized by attaching a photolabile cross-linking group, such as aryliazirine and arylazido, and an indicator tag such as biotin to the ligand (27). However, the incorporation of a bulky tag often causes a significant decrease in the ligand's affinity for the target. The steric hindrance due to the incorporation of a tag can be overcome by introducing a radioisotope, whereas the incorporation of a photolabile group is crucial. Therefore, to avoid a significant decrease in affinity, the photolabile group is generally introduced at a position remote from a toxophoric moiety and inherently unessential for exhibiting high affinity.

Actually, the same holds true for the photoaffinity inhibitor probes used in researching complex I. In earlier photoaffinity labeling studies using pyridaben (21) and fenpyroximate (22) derivatives, a photolabile aryliazirine group was attached to the moiety where it is remote from the toxophoric heterocyclic ring and merely enhances the hydrophobicity of the molecule. However, this strategy in the compound design has fundamental problems: (i) the region cross-linked by the photolabile group may not be responsible for critical interaction with the inhibitor and hence for important functionality of the enzyme and (ii) the unessential moiety of the inhibitor may be too flexible to fix the position of a photolabile group in the enzyme. In fact, some phenomena that would be associated with these problems can be observed in early photoaffinity labeling studies. For instance, a pyridaben derivative predominantly bound to the PSST subunit, but with significant nonspecific binding to the ND1 subunit (21). A fenpyroximate derivative bound to the ND5 subunit (22). This subunit is however suggested to be located far from the peripheral arm, i.e., at the distal end of the membrane arm (28, 29).

It would therefore be ideal if some photoreactive group could substitute for a toxophoric core structure with no loss of function. Although this idea seems unrealistic at first sight, several examples of photoaffinity probes are of particular interest. For instance, by synthesizing a photoreactive analogue of retinal in which the β -ionone ring was substituted with a photoreactive diazo ketone, Nakanishi and colleagues succeeded in identifying the amino acid residues binding 11-*cis*-retinal before the crystal structure of rhodopsin was available (30). We have synthesized a photolabile acetogenin derivative ($[^{125}\text{I}]JTDA$) in which an aryliazirine group serves as a substitute for the toxophoric γ -lactone ring as well as a photoreactive group (23). Using this inhibitor probe, we revealed that the acetogenin binds to the ND1 subunit with high specificity (23). Although the ND1 has been implicated in the proton-pumping activity of bovine complex I (31, 32), our study unequivocally revealed that it is one of the subunits constructing the inhibitor binding domain.

Quinazoline-type chemicals are strong inhibitors of bovine heart mitochondrial complex I and highly fluorescent (14, 15). In the present study, we focused our attention on quinazolines as test compounds for two reasons. First, on the basis of competition experiments taking advantage of a partial quenching of the fluorescence of quinazolines upon specific binding to complex I, it was suggested that a variety of

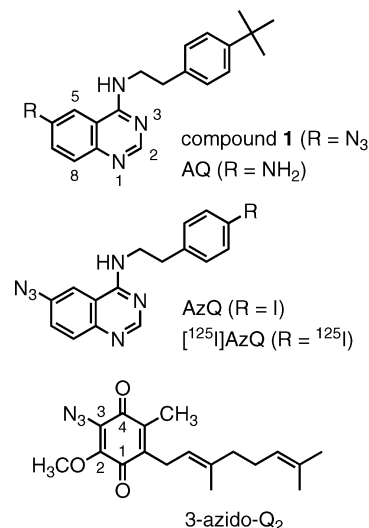


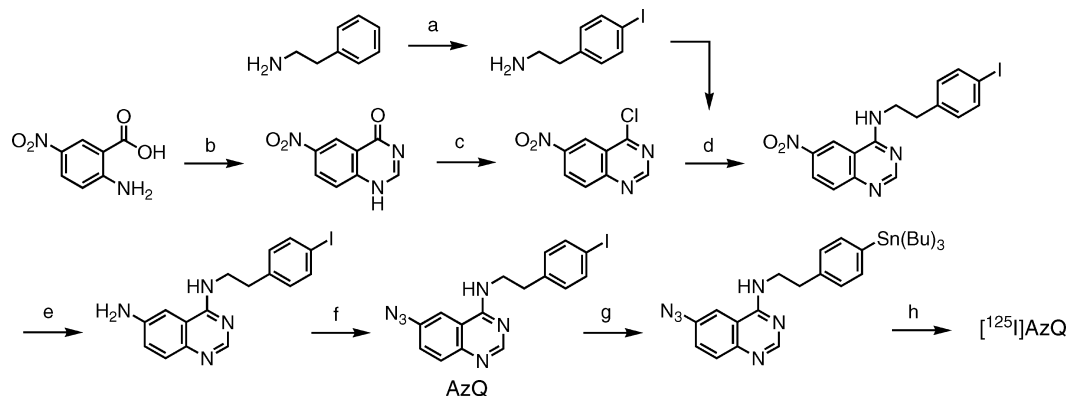
FIGURE 1: Structure of quinazoline-type inhibitors examined in this study and 3-azido-ubiquinone-2.

complex I inhibitors share a common binding domain (14, 15). Second, an azido derivative of quinazoline (compound 1, Figure 1), which possesses a photolabile azido group *on the toxophoric quinazoline ring*, maintains a strong inhibitory effect on bovine complex I (33) and hence is suitable as a candidate photoaffinity probe, as described above. Thus identification of the binding site of quinazolines is important for elucidating the inhibitor binding site in complex I. We here synthesized a ^{125}I -labeled azidoquinazoline (6-azido-4-(4-iodophenethylamino)quinazoline, AzQ, Figure 1) and carried out photoaffinity labeling experiments with bovine complex I. Our study revealed that $[\text{^{125}\text{I}}]\text{AzQ}$ specifically binds to the 49 kDa and ND1 subunits with a frequency of $\sim 4:1$. The combination of different proteolysis of the cross-linked 49 kDa subunit indicated the binding site of $[\text{^{125}\text{I}}]\text{AzQ}$ to be located within the region Asp41–Arg63 (23 amino acids). The present study has revealed, for the first time, the inhibitor binding site in complex I at the sub-subunit level.

EXPERIMENTAL PROCEDURES

Materials. Bullatacin and piericidin A were kindly provided by Drs. J. L. McLaughlin (Purdue University, West Lafayette, IN) and S. Yoshida (The Institute of Physical and Chemical Research, Saitama, Japan), respectively. Rabbit anti-ND1 antibody was a generous gift from Dr. T. Yagi (The Scripps Research Institute, La Jolla, CA). Ubiquinone-1 (Q₁) and -2 (Q₂) were kindly provided by Eisai Co. (Tokyo, Japan). 6-Amino-4-(4-*tert*-butylphenethylamino)quinazoline (AQ) was the same sample used previously (15). Protein standards (Precision Plus Protein Standards and Kaleidoscope Polypeptide Standards) for SDS-PAGE were purchased from Bio-Rad (Hercules, CA). $[\text{^{125}\text{I}}]\text{NaI}$ was purchased from Perkin-Elmer (Waltham, MA). Rat monoclonal anti-30 kDa subunit (in complex I) and ADP/ATP carrier antibodies were from MitoSciences (Eugene, OR). Other reagents were all of analytical grade.

Synthesis of AzQ and $[\text{^{125}\text{I}}]\text{AzQ}$. The procedures used to produce photoreactive AzQ and its ^{125}I -labeled derivative ($[\text{^{125}\text{I}}]\text{AzQ}$) are outlined in Scheme 1. The radiochemical yield from the initial $[\text{^{125}\text{I}}]\text{NaI}$ was 65%, and the specific radioactivity was 2000 Ci/mmol. Radiochemical purity was

Scheme 1^a

^a Reagents and reaction conditions: (a) (i) (CF₃CO)₂O, CH₂Cl₂, 4 °C, 1 h, (ii) I₂, Ph(OCOCF₃)₂I, room temperature, 15 h, (iii) 15% NaOH, CH₃OH, room temperature, 1 h, 34% (3 steps); (b) HCONH₂, 140 °C, 6 h, 73%; (c) PCl₅, POCl₃, 110 °C, 5 h; (d) (Et)₃N, benzene, 80°C, 12 h, 30% (2 steps); (e) Fe, CH₃COOH, H₂O-EtOH (2:3), reflux, 4 h, 60%; (f) i) NaNO₂, H₂O/MeOH/HCl (2:1:1), 4 °C, 1 h, ii) NaN₃, 4 °C, 74% (2 steps); (g) hexabutyltin, Pd(PPh₃)₄, dioxane, 50 °C, 12 h, 15%; (h) [125I]NaI (2000 Ci/mmol), chloramine T, aqueous NaH₂PO₄ (0.2 M).

examined by HPLC and silica gel TLC (thin-layer chromatography) and determined to be over 99%. Synthetic details and spectral data for the compounds are described in the Supporting Information.

Preparation of Bovine Submitochondrial Particles and Enzyme Assays. Mitochondria were isolated from bovine heart (34). Submitochondrial particles (SMP) were prepared by the method of Matsuno-Yagi and Hatefi (35) using a sonication medium containing 250 mM sucrose, 1 mM succinate, 1.5 mM ATP, 10 mM MgCl₂, 10 mM MnCl₂, and 10 mM Tris-HCl (pH 7.4) and stored in a buffer containing 250 mM sucrose and 10 mM Tris-HCl (pH 7.4) at -80 °C until use. NADH oxidase activity in SMP was measured spectrometrically with a Shimadzu UV-3000 (340 nm, $\epsilon = 6.2 \text{ mM}^{-1} \text{ cm}^{-1}$) at 30 °C. The reaction medium (2.5 mL) contained 250 mM sucrose, 1 mM MgCl₂, and 50 mM KP_i buffer (pH 7.4), and the final protein concentration was 30 µg/mL. The reaction was started by adding 50 µM NADH after the equilibration of SMP with an inhibitor for 4 min. NADH-Q₁ activity was measured under the same experimental conditions, except that the reaction medium contained 50 µM Q₁, 0.2 µM antimycin A, and 2 mM KCN.

The activities of ADP/ATP carrier and 3-hydroxybutyrate dehydrogenase in SMP were determined as described by Majima et al. (36) and McIntyre et al. (37), respectively.

Photoaffinity Labeling of SMP by [125I]AzQ. Bovine SMP (0.3–1.0 mg of protein/mL, 100 µL in a 1.5 mL tube) were incubated with [125I]AzQ (3–10 nM) in a buffer containing 250 mM sucrose, 1 mM MgCl₂, and 50 mM KP_i (pH 7.4) for 10 min at room temperature. Then, the samples were irradiated for 10 min with a long-wavelength UV lamp (Black Ray model B-100A, UVP, Upland, CA) on ice at a distance of 15 cm from the light source. When the competition was examined, a competitor was added and incubated for 10 min at room temperature prior to treatment with [125I]AzQ.

1D Electrophoresis. Sodium dodecyl sulfate–polyacrylamide gel electrophoresis (SDS-PAGE) was performed according to Laemmli (38). Briefly, photoaffinity-labeled samples were added to 4× Laemmli's sample buffer and incubated at 35 °C for 1 h. These denatured samples were separated on 12.5% gels. After electrophoresis, the gels were

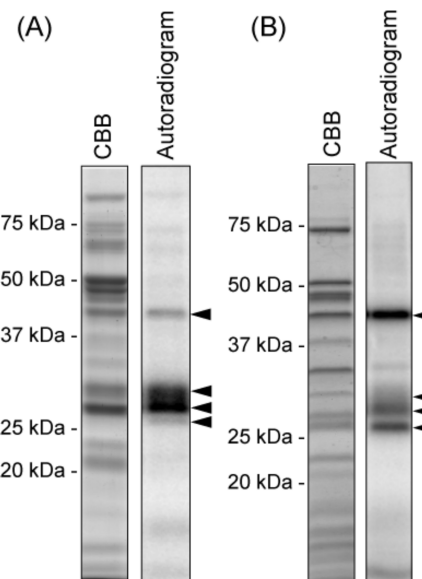


FIGURE 2: SDS-PAGE analysis of [125I]AzQ-labeled SMP and electroeluted complex I. (A) Bovine heart SMP (0.3 mg of protein/mL) were photo-cross-linked by [125I]AzQ (3 nM) according to the Experimental Procedures and analyzed by SDS-PAGE on a 12.5% SDS gel. Proteins were visualized by CBB and subjected to autoradiography. (B) Complex I was electroeluted from BN-PAGE of SMP (1.0 mg of protein/mL) cross-linked by [125I]AzQ (10 nM). Proteins were resolved on a 12.5% SDS gel and subjected to CBB staining and autoradiography.

stained with Coomassie brilliant blue R-250 or silver (silver stain MS kit; Wako Pure Chemical Industries, Osaka, Japan) and exposed to an imaging plate (BAS-MS2040; Fuji Film, Tokyo, Japan). The migration pattern of radiolabeled proteins was analyzed and visualized with a bio-imaging analyzer FLA-5100 (Fuji Film). The radioactivity of each band was quantified from the digitalized data using "Multi Gauge" software (Fuji Film) or directly from the dried gel slices using a γ -counting system (COBLA II; Packard).

Analytical blue native (BN)-PAGE (analytical scale) was performed using the native PAGE Novex Bis-Tris gel system with a 4–16% precast gel (Invitrogen, Carlsbad, CA), according to the manufacturer's protocol. Electrophoresis was performed at a voltage of 150 V with a limited current of 15 mA/gel in a cold room. After electrophoresis, the complex I band

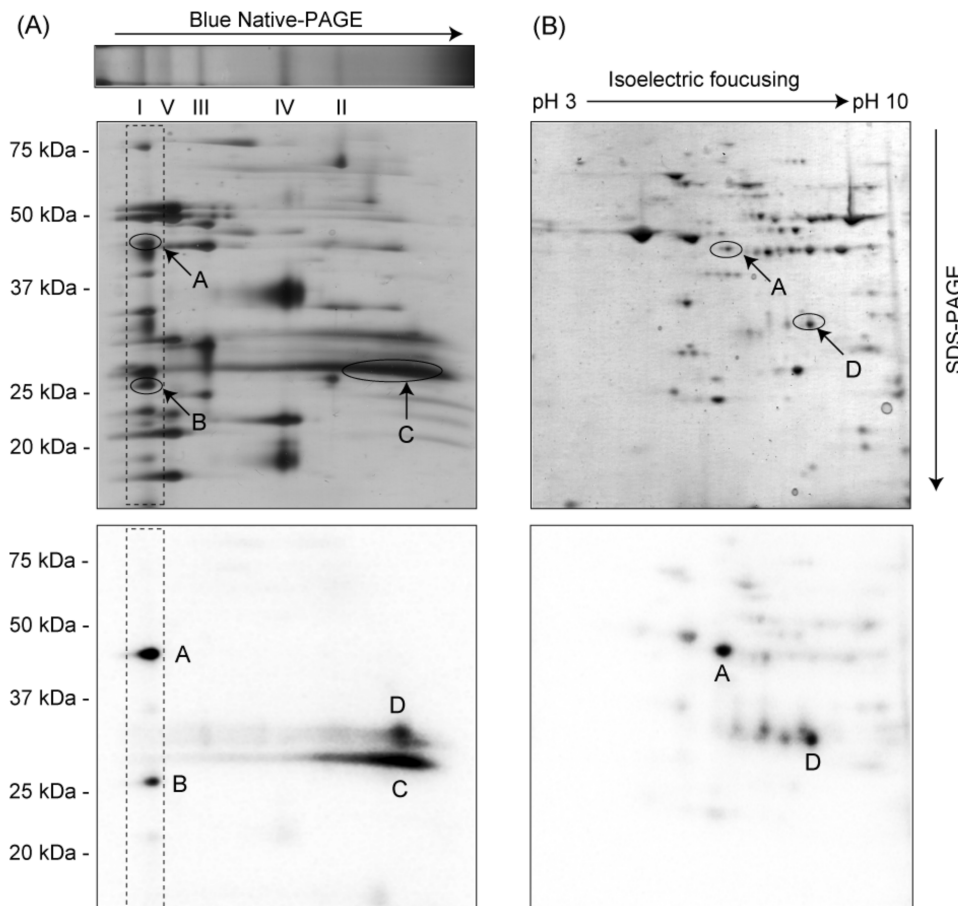


FIGURE 3: Resolution of [^{125}I]AzQ-labeled SMP by 2D electrophoresis. Bovine heart SMP (1.0 mg of protein/mL) were photoaffinity labeled with [^{125}I]AzQ (10 nM) and resolved by two different types of 2D electrophoresis. (A) BN/SDS-PAGE. The labeled SMP (20 μg) were separated on a 4–16% BN gel in the first dimension. Lanes were excised from the BN gel and subjected to SDS-PAGE on a 12.5% Laemmli's gel in the second dimension. Proteins were visualized by silver staining (upper) and subjected to autoradiography (lower). The dotted lane indicates the components of complex I. (B) IEF/SDS-PAGE. The labeled SMP (80 μg) were separated by IEF on an immobilized pH gradient strip (pH 3–10, first dimension), followed by SDS-PAGE (second dimension). Proteins were visualized by CBB (upper) and autoradiographed (lower). Letters show the spots identified by peptide mass fingerprinting as the binding proteins of [^{125}I]AzQ: spot A, 49 kDa subunit (complex I); spot B, ND1 subunit (complex I); spot C, ADP/ATP carrier; spot D, 3-hydroxybutyrate dehydrogenase.

was identified by staining “in-gel” activity with the NADH/NBT system (39) and autoradiographed as described above. Preparative BN-PAGE was performed using a 6% isocratic hand-cast gel ($160 \times 180 \times 2$ mm), and complex I was isolated by electroelution as described procedures (23, 40). The complex I obtained was stored at -80°C until use.

2D Electrophoresis. For the isoelectric focusing (IEF)/SDS 2D analysis, first dimensional IEF was carried out using the IPGphor system (GE Healthcare, Buckinghamshire, U.K.) with an Immobiline DryStrip (7 cm, pH 3–10, GE Healthcare). Prior to loading of the proteins, labeled SMP (solubilized in 1% SDS) and complex I electroeluted by BN-PAGE were precipitated with a 2D-CleanUp Kit (GE Healthcare) according to the manufacturer's protocols. The precipitated proteins were solubilized in a rehydration buffer containing 7 M urea, 2 M thiourea, 4% CHAPS, 0.5% IPG buffer, 40 mM DTT, and 0.002% BPB. Immobilized pH gradient strips were rehydrated in 125 μL of the rehydration buffer containing mitochondrial proteins for 12–20 h at 20°C and 20 V, followed by successive voltages of 300 V (30 min, step), 1000 V (30 min, gradient), 5000 V (1 h 20 min, gradient), and 5000 V (1 h, step). After IEF was completed, the strips were reduced with 5 mL of equilibration buffer (50 mM Tris-HCl, 6 M urea, 1% SDS, 30% glycerol, a trace of BPB, pH 8.8) containing 0.25% (w/v) DTT for 10 min

and alkylated with 5 mL of the same equilibration buffer containing 4.5% (w/v) iodoacetamide. The treated strips were subjected to a second dimensional analysis using Laemmli's 12.5% SDS gel. The protein spots were visualized with CBB R-250 or silver (silver stain MS kit; Wako) and subjected to autoradiography.

For the BN/SDS 2D analysis, first dimensional BN-PAGE was performed on a 4–16% precast gel (Invitrogen) as described above. After BN-PAGE was completed, one lane was excised and denatured in the same way as the IEF strip and subjected to a second dimensional analysis on Laemmli's gel.

Immunochemical Analysis. Electrophoresed mitochondrial protein or complex I was electroblotted onto a PVDF membrane (Immn-blot PVDF membrane, 0.2 μm ; Bio-Rad, Hercules, CA) in a buffer containing 10 mM NaHCO₃, 3 mM Na₂CO₃, and 0.025% (w/v) SDS overnight at 35 V (100 mA) in a cold room (41). The blotted membrane was blocked with 1% gelatin in Tween TBS (10 mM Tris-HCl, pH 7.4, 0.9% NaCl, and 0.05% Tween 20) for 1 h at room temperature. In the case of the anti-ADP/ATP carrier monoclonal antibody, the blocking solution provided and Tween PBS were used. The blocked PVDF membrane was probed with primary antibodies for 1 h at room temperature and then incubated for another 1 h with AP-conjugated

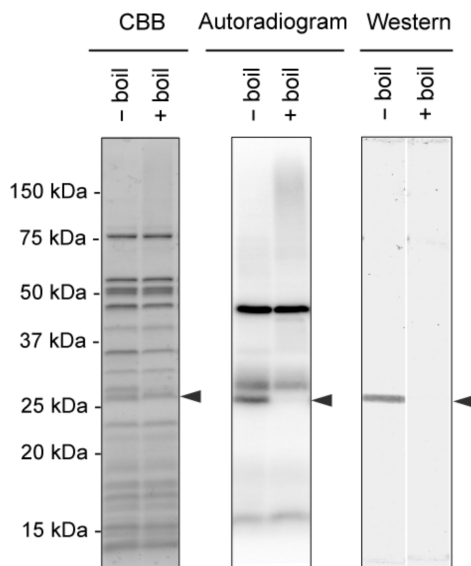


FIGURE 4: Effect of heating on resolution of the ND1 subunit with SDS-PAGE. The [125 I]AzQ-labeled complex I was analyzed on a 12.5% Laemmli's gel (equivalent to 50 μ g of SMP protein/well). The samples were treated with a Laemmli's SDS-PAGE sample buffer and incubated at 35 °C for 1 h (−boil) or heated at 95 °C for 5 min (+boil). After the electrophoresis, proteins were visualized by CBB, autoradiographed, and subjected to the Western blotting using anti-bovine ND1 antibody.

secondary antibodies (Daiichi Pure Chemicals, Tokyo, Japan) at room temperature. The treated membrane was washed with Tween TBS (10 min \times 3 times) and developed with NBT/BCIP chromogenic substrates (AP color development kit; Bio-Rad).

Mass Spectrometric Analysis. Radioactive gel spots were identified by peptide mass fingerprinting at the APRO Life Science Institute, Inc. (Tokushima, Japan) with a Voyager-DE STR (MALDI-TOF MS system; Applied Biosystems, Foster City, CA). Each gel spot identified by CBB or silver staining was in-gel digested by trypsin, and the extracted peptides were subjected to MALDI-TOF MS. The spectra were scanned in the reflector and positive-ion mode from 800 to 4000 (m/z) and externally calibrated with des-Arg¹-bradykinin (m/z 904.4681), angiotensin I (m/z 1296.6853), Glu¹-fibrinopeptide B (m/z 1570.6744), ACTH (clip 1–17, m/z 2093.0867), and ACTH (clip 18–39, m/z 2465.1989). α -Cyano-4-hydroxycinnamic acid was used as a matrix. Obtained monoisotopic masses were compared against NCBInr databases (*Bos taurus*) using the MASCOT program (<http://www.matrixscience.com>), with a peptide mass tolerance of 20 ppm and maximum missed cleavage of 1. The calbamidomethylation of cysteine residues and oxidation of methionine residues were set to variable modifications.

Limited Proteolysis of the 49 kDa Subunit. Peptide mapping of the 49 kDa subunit was carried out according to the Cleveland method (42) with some modifications by Omori et al. (43). Complex I isolated from the BN-PAGE gel was separated on a 12.5% SDS gel. The CBB-stained 49 kDa subunit was excised and subjected to digestion by V8-protease in an EDTA-containing 15% mapping gel (90 \times 80 \times 1 mm). Prior to the insertion of the gel pieces, 1 μ g of V8-protease was loaded into each well and buried in the stacking gel by preelectrophoresis. The V8 digestion was carried out at the boundary between the stacking gel and the separating gel for 30 min at room temperature. After

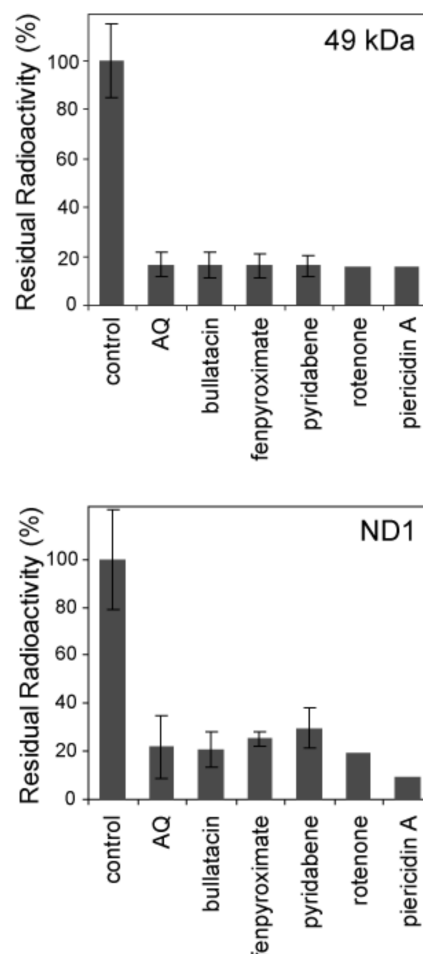


FIGURE 5: Suppression of cross-linking of the 49 kDa and ND1 subunits by other inhibitors. Bovine SMP (1.0 mg of protein/mL) were cross-linked by [125 I]AzQ (5 nM) in the presence of various complex I inhibitors at 1.0 μ M (200-fold). SMP were solubilized with 1% (w/v) DDM and separated by BN-PAGE (4–16%). The complex I band was cut out from the gel and subjected to second dimensional SDS-PAGE on a 12.5% Laemmli's gel. Residual radioactivity in the 49 kDa and ND1 subunits is indicated. The averaged control radioactivity in the 49 kDa and ND1 bands is 660 (\pm 100) and 180 (\pm 37) cpm, respectively. Data are the means of three independent measurements \pm the standard deviation, but the data for rotenone and piericidin A are from a single experimental run.

electrophoresis, partially digested peptides on the SDS gel were transferred onto a PVDF membrane (Immobilon-P^{SO}; Millipore, Billerica, MA) and identified by CBB staining and autoradiography. The radioactive bands were subjected to the N-terminal sequence analysis using the Procise 494 HT and 494 cLC protein sequencing system (Applied Biosystems).

For complete digestion of the 49 kDa subunit, [125 I]AzQ-labeled SMP were partially purified by SDS-PAGE on 12.5% Laemmli's gel, and the radioactive area around the subunit was excised. The gel slices containing the [125 I]AzQ-labeled 49 kDa subunit were subjected to electroelution using a Centricon equipped with a Centricon YM-10 (Millipore). Typically, more than 80% of the radioactivity was recovered from the gel. The isolated 49 kDa subunit was digested with V8-protease (Roche Applied Science, Penzberg, Germany), lysylendopeptidase (Lys-C; Wako Pure Chemicals), or trypsin (Promega, Madison, WI) in 50 mM ammonium bicarbonate buffer (pH 7.8), 20 mM Tris-HCl buffer (pH

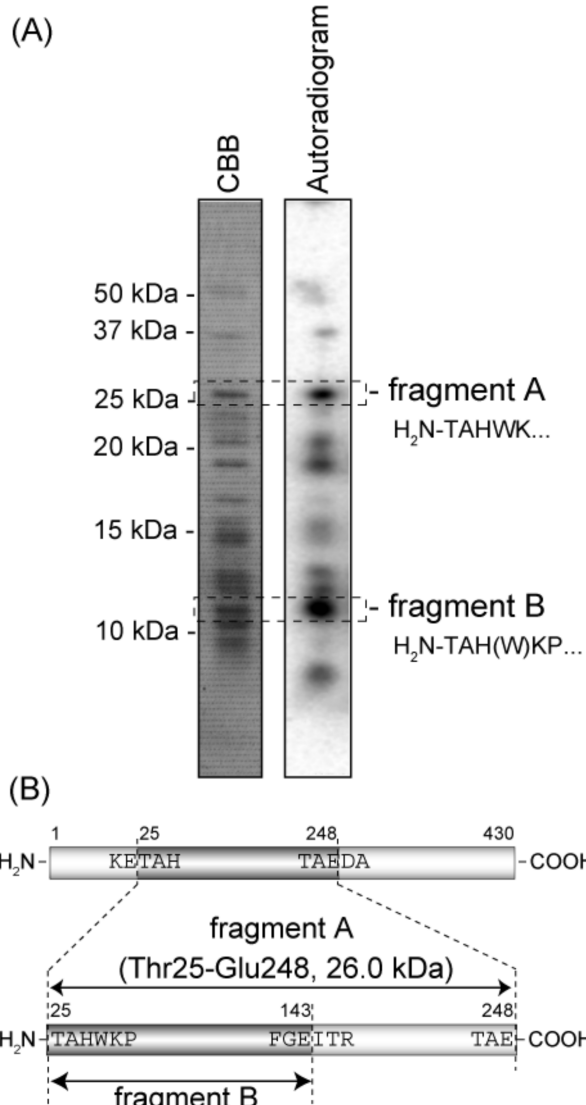


FIGURE 6: Proteolytic mapping of the 49 kDa subunit with V8-protease. The [¹²⁵I]AzQ-labeled complex I (equivalent to 400 μ g of SMP protein/well) was separated on a 12.5% Laemmli's gel. The CBB-stained 49 kDa subunit was transferred to the 15% mapping gel and subjected to partial digestion with V8-protease (1 μ g/well). (A) Electrophoresed digests were transferred to PVDF membrane and stained by CBB and autoradiographed. From fragments A and B, the indicated N-terminal sequences were obtained. (B) A schematic presentation of proteolytic mapping of the 49 kDa subunit. Residue numbers refer to the mature sequence of the 49 kDa subunit (P17694) in bovine complex I.

9.0), or 50 mM Tris-HCl buffer (pH 8.5), respectively. Protease/substrate ratios were set to 1/30–1/15, and the digestion was continued overnight at 37 °C. The digests were lyophilized and further analyzed by reverse-phase HPLC or tricine-SDS-PAGE (16.5% T/6% C; ref (44)).

Bioinformatics Studies. Sequence alignments were performed using the Clustal W program. GenBank accession numbers of the 49 kDa sequences of representative organisms are as follows: *B. taurus* (bovine) 49 kDa (P17694), *Y. lipolytica* 49 kDa (XP_505527), *Paracoccus denitrificans* Nqo4 (P29916), *T. thermophilus* Nqo4 (Q56220), and *Escherichia coli* NuoC/D (P33599). The crystal structure of the peripheral arm from *T. thermophilus* was obtained from the Protein Data Bank in the PDB format (PDB code: 2FUG) and visualized using Mac PyMOL software (version 0.99,

downloaded from <http://pymol.org/>). The mobility shifts of enzymatic digests on tricine gel were predicted using Peptide Mass (<http://expasy.org/tools/peptide-mass.html>) and Peptide Cutter (<http://expasy.org/tools/peptidecutter/>).

RESULTS

Synthesis and Characterization of [¹²⁵I]AzQ. We previously showed that an azido derivative of quinazoline (compound **1**) exhibits a potent inhibitory effect on bovine complex I at the nanomolar level (33). To synthesize a photoaffinity labeling probe by introducing ¹²⁵I-label, we tried to substitute a *tert*-butyl group of compound **1** with an iodine, giving AzQ (Figure 1). The inhibitory effect of AzQ was examined with NADH oxidase activity in SMP (30 μ g of protein/mL). The IC₅₀ values of compound **1** and AzQ were 2.3 (\pm 0.3) and 4.5 (\pm 0.6) nM, respectively, indicating that AzQ is slightly less active due to less hydrophobicity (*tert*-butyl vs iodine) but still has a potent inhibitory effect. We therefore chose AzQ as a photoaffinity labeling probe and synthesized ¹²⁵I-labeled AzQ ([¹²⁵I]AzQ, ~2000 Ci/mmol).

Photoaffinity Labeling of Bovine SMP by [¹²⁵I]AzQ. For photoaffinity labeling, SMP were used to ensure the intactness of complex I (21). UV irradiation of SMP (0.3 mg of protein/mL) in the presence of [¹²⁵I]AzQ (3 nM) resulted in four photo-cross-linked bands on the 1D SDS gel (Figure 2A). Nearly complete labeling (>90%) was established within 10 min of UV irradiation. When complex I was isolated by electroelution from the BN-PAGE gel, the relative intensity of ~45 and ~25 kDa bands remarkably increased (Figure 2B). These results mean that [¹²⁵I]AzQ also cross-linked to mitochondrial proteins which are not components of complex I.

In order to characterize each band cross-linked by [¹²⁵I]-AzQ, we tried to resolve bovine SMP proteins by two types of different 2D electrophoresis, i.e., BN/SDS-PAGE and IEF/SDS-PAGE. BN/SDS-PAGE is an efficient method for the analysis of mitochondrial respiratory complexes (45, 46). As shown in Figure 3A (upper), photoaffinity-labeled SMP were solubilized in 1% DDM, and five respiratory complexes were separated on the first dimensional BN gel. After separation on the BN gel, the excised lane was subjected to second dimensional SDS-PAGE. Components of the five respiratory complexes were separated in vertical lanes in Figure 3A. Figure 3A (lower) shows an autoradiograph of the BN/SDS gel. Radioactivity was distributed into two spots (spots A and B) with a frequency of ~4:1 in the vertical lane consisting of complex I subunits and two other spots (spots C and D). Spots C and D were not resolved as clear bands on the first dimensional BN-PAGE gel. These results show that [¹²⁵I]AzQ cross-links to two proteins in complex I and two additional proteins which are not components of complex I. Since spot D was markedly unclear and difficult to identify on the silver-stained BN/SDS gel, we separated it on a conventional IEF/SDS gel (Figure 3B). Spots B and C on the BN/SDS gel (Figure 3A) were not detected on the IEF/SDS gel, suggesting that both spots were highly hydrophobic proteins (47).

Thus we succeeded in visualizing the labeling pattern of [¹²⁵I]AzQ by using two different 2D gels. To identify the [¹²⁵I]AzQ-labeled proteins, nonradioactive spots on the 2D gels (i.e., spots A, B, and C on the BN/SDS gel and spot D

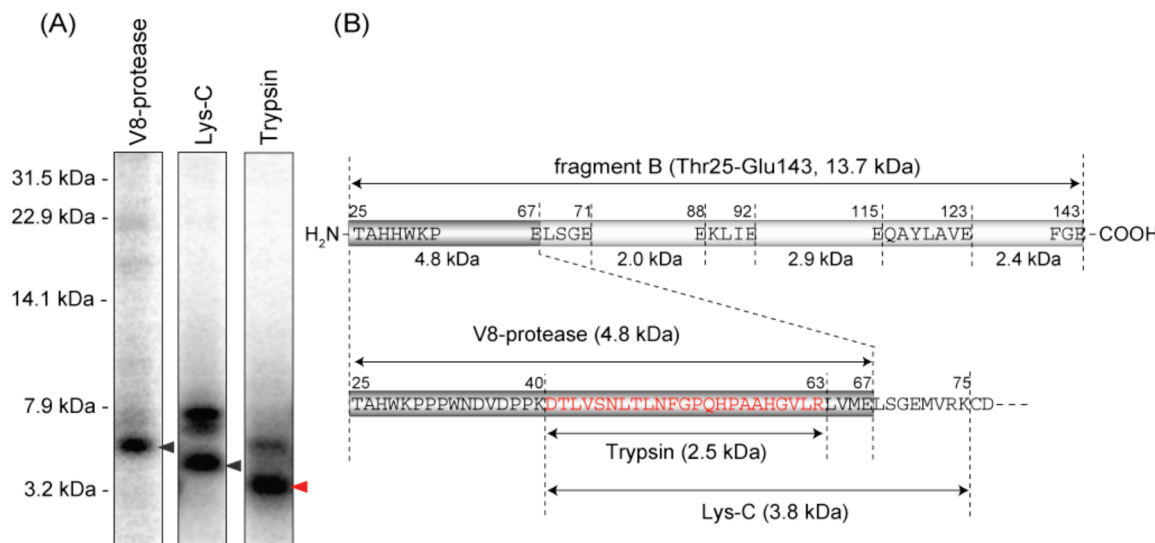


FIGURE 7: Exhaustive digestion of the 49 kDa subunit by V8-protease, Lys-C, or trypsin. The [¹²⁵I]AzQ-labeled 49 kDa subunit was purified by Laemmli's SDS-PAGE and electroelution. The isolated protein was digested with V8-protease, Lys-C, or trypsin as described in the Experimental Procedures. (A) Proteolytic digests were separated by tricine/SDS-PAGE (16.5% T/6% C) and autoradiographed. (B) A schematic presentation of proteolytic mapping of fragment B (Thr25–Glu143).

on the IEF/SDS gel) were subjected to in-gel tryptic digestion and peptide mass fingerprinting by MALDI-TOF MS. The mass spectrometric analysis revealed that the labeled proteins are the 49 kDa (spot A, 59% sequence coverage) and ND1 (spot B, 15%) subunits in complex I and ADP/ATP carrier (spot C, 40%) and 3-hydroxybutylate dehydrogenase (spot D, 48%) (Table S1 of the Supporting Information). The apparent pI of 3-hydroxybutylate dehydrogenase on IEF/SDS gel was somewhat consistent with the predicted value (8.9), and the mobility shift of ADP/ATP carrier on the BN/SDS gel was also examined by Western blotting (Figure S2 of the Supporting Information). While we examined the effect of AzQ (up to 20 μ M) on the activities of both ADP/ATP carrier and 3-hydroxybutylate dehydrogenase, the binding of AzQ was not associated with dysfunction of the two proteins; therefore, we did not investigate these proteins further.

In spot B, we also observed tryptic digests derived from the 30 kDa subunit of complex I. However, we exclude the possibility that [¹²⁵I]AzQ binds to this subunit for the following reasons: first, the 30 kDa subunit is located in the upper position of the ND1 subunit on the 12.5% Laemmli's gel (confirmed by the Western analysis), and second, the 30 kDa subunit can be resolved on the 2D (IEF/SDS) gel (confirmed by the Western analysis and also see ref 48).

Using complex I isolated by electroelution from the BN-PAGE gel, we obtained similar migration patterns of the labeled 49 kDa subunit on the 1D and 2D (IEF/SDS) gels and the ND1 subunit on the 1D gel (Figure S3 of the Supporting Information). The mobility shift of the 49 kDa subunit and disappearance of the ND1 subunit on the 2D gel are consistent with the observation made by Carroll et al. (48). In addition, when the samples were boiled for 4 min before SDS-PAGE, the CBB-stained ND1 band and the radioactivity on the SDS gel disappeared (Figure 4), as mentioned in ref 23. It should be noted that a close correlation was found between the incorporation of the radioactivity into the 49 kDa and ND1 subunits and the inhibition

of NADH oxidase activity (Figure S4 of the Supporting Information).

Effect of Other Complex I Inhibitors on [¹²⁵I]AzQ Labeling. Previous photoaffinity labeling studies revealed that pyridaben, fenpyroximate, and acetogenin analogues specifically bind to the PSST, ND5, and ND1 subunit, respectively (21–23). These bindings were suppressed in the presence of excess amounts of other complex I inhibitors. We therefore examined whether the labeling of the 49 kDa and ND1 subunits by [¹²⁵I]AzQ is suppressed by other inhibitors. Including a strong quinazoline-type inhibitor AQ, other inhibitors (bulatacin, fenpyroximate, pyridaben, rotenone, and piericidin A) markedly suppressed the labeling of both subunits at a concentration of 1 μ M (200-fold), as shown in Figure 5. The simplest interpretation of these results is that all inhibitors examined share a large common binding domain, being consistent with the concept proposed by Okun et al. (14). Nevertheless, on the basis of a mechanistic study on novel piperazine-type inhibitors (49), we recently proposed that the apparent competitive behavior among various complex I inhibitors does not necessarily mean the occupation of the same binding site but rather is due to structural change at the binding site induced by a competitor.

It is noteworthy that an excess amount of other inhibitors, except AQ having the same core structure, did not suppress the cross-linking of ADP/ATP carrier and 3-hydroxybutylate dehydrogenase by [¹²⁵I]AzQ.

Effect of Short-Chain Ubiquinones on [¹²⁵I]AzQ Labeling. Although various complex I inhibitors are generally believed to act at the ubiquinone reduction site, there is still no hard experimental evidence to verify this. Rather, photoaffinity labeling studies using photoreactive ubiquinones suggested that the inhibitor binding site is not the same as the ubiquinone reduction site (12, 13). We therefore examined the suppression effect of Q₂ (K_m = 3 μ M, ref 50) on the cross-linking of [¹²⁵I]AzQ (3 nM) to the 49 kDa and ND1 subunits. At a concentration of 30 μ M (10000-fold), being nearly the solubility limit, Q₂ suppressed the cross-linking of both subunits by only 10–20%. We also carried out the

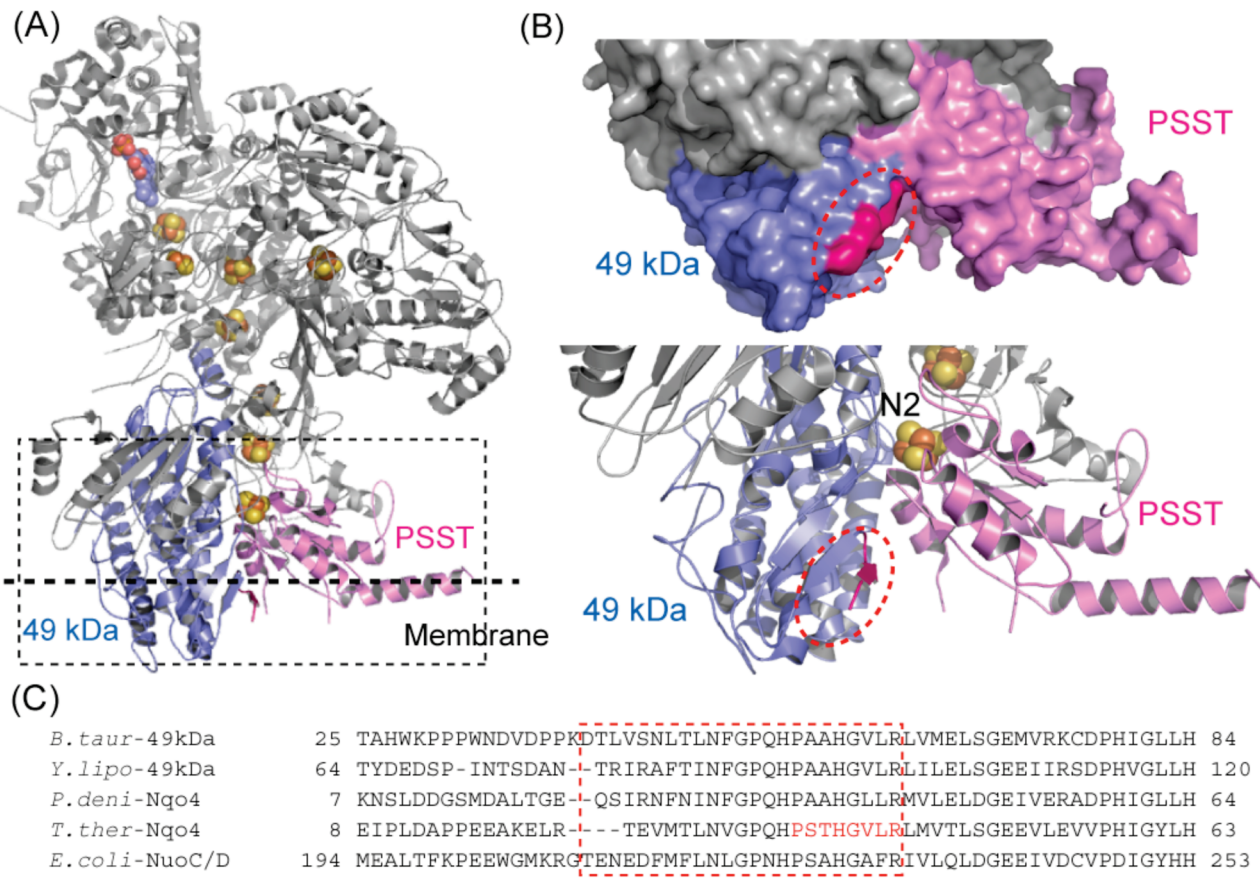


FIGURE 8: The binding site of [¹²⁵I]AzQ in complex I. (A) The crystal structure of the peripheral arm of complex I from *T. thermophilus* (3). Nqo4 (49 kDa) and Nqo6 (PSST) in magenta). (B) Close-up of the Nqo4 and Nqo6 subunits. As some N-terminal residues in the sequence corresponding to the labeled region Asp41–Arg63 in bovine were not modeled in the crystal structure due to lack of electron density (3), only the resolved region Pro35–Arg42, which corresponds to Pro56–Arg63 in bovine, is shown in red. (C) Amino acid sequence alignment of the 49 kDa subunit from various organisms. The sequence corresponding to Asp41–Arg63 in bovine is surrounded by a dotted red line. In *T. thermophilus* Nqo4, the region Pro35–Arg42 modeled in the crystal structure is shown in red.

competition test using a photoreactive 3-azido-Q₂ ($K_m = 5 \mu\text{M}$, Figure 1), which is able to cross-link to the enzyme by UV irradiation, as demonstrated with the cytochrome *bd* complex from *E. coli* (51). 3-Azido-Q₂ also suppressed the cross-linking by just 10–20% at 30 μM (10000-fold).

These results cannot be simply interpreted to mean that [¹²⁵I]AzQ does not bind to the ubiquinone reduction site because (i) the competition experiment between [¹²⁵I]AzQ and an exogenous short-chain ubiquinone is virtually impractical since the binding affinities of the two ligands are too different (about 3 orders of magnitude) to examine efficient competition behavior in a limited concentration range and (ii) high concentrations of hydrophobic chemicals (i.e., ubiquinones) accumulated in SMP may alter the properties of membrane proteins in a nonspecific manner.

Analysis of the Cross-Linked Region of [¹²⁵I]AzQ in the 49 kDa Subunit. According to the crystal structure of the peripheral arm of complex I from *T. thermophilus*, the Nqo4 (49 kDa in bovine) and Nqo6 (PSST), which contains a terminal Fe–S cluster N2, subunits are believed to construct the quinone binding cavity. On the basis of site-directed mutagenesis studies in *Y. lipolytica*, Brandt and colleagues suggested that the 49 kDa subunit comprises the ubiquinone/inhibitor binding domain (19, 52). Thus, the 49 kDa subunit is a key component of complex I in terms of the function of the enzyme.

We therefore tried to identify the binding region of [¹²⁵I]AzQ in the 49 kDa subunit by limited proteolysis. The [¹²⁵I]AzQ-labeled complex I was separated on a SDS gel, and the Coomassie stained 49 kDa subunit was excised from the gel and subjected to partial digestion using V8-protease. This proteolytic mapping experiment reproducibly produced two major radioactive bands at ~28 (fragment A) and ~13 kDa (fragment B) on the SDS gel and PVDF membrane (Figure 6A). When the sample was digested by a large amount of V8-protease, the radioactivity shifted to fragment B. These results indicate that [¹²⁵I]AzQ was incorporated into fragment B, which is a further digest of fragment A.

The N-terminal sequencing of the two bands provided partial amino acid sequences: NH₂-TAHWK- and NH₂-TAH(W)KP- for fragments A and B, respectively. Considering the apparent molecular mass of these bands on the SDS gel and theoretical cleavage sites of V8-protease, fragment A is predicted to be the peptide Thr25–Glu248 (224 amino acids, 26.0 kDa), which was further cleaved at Glu143 and gave fragment B (Thr25–Glu143, 118 amino acids, 13.7 kDa). A summary of the digestion map of the [¹²⁵I]AzQ-labeled 49 kDa subunit is shown in Figure 6B.

To further localize the cross-linked site of [¹²⁵I]AzQ, the 49 kDa subunit isolated from the SDS gel was exhaustively digested by V8-protease, Lys-C, or trypsin (Figure 7A). Exhaustive digestion of the [¹²⁵I]AzQ-labeled 49 kDa subunit

by V8-protease revealed the migration of a radioactive band with an apparent molecular mass of ~5 kDa on the tricine gel. Careful analysis of the cleavable site of V8-protease in the region of fragment B provided the sequence Thr25–Glu67 with a calculated molecular mass of 4.8 kDa (Figure 7B). Similar digestion using Lys-C and trypsin gave a radioactive band at ~4 and ~3 kDa, respectively (Figure 7A). Reverse-phase HPLC resolution of the tryptic digests of the [¹²⁵I]AzQ-labeled 49 kDa subunit resulted in one major photo-cross-linked peak, which is thought to be the ~3 kDa band on the SDS gel (Figure S5 of the Supporting Information). This result strongly suggests the presence of one [¹²⁵I]AzQ-labeled site in the peptide fragment with high specificity. Along with the result of V8-protease digestion, examination of the cleavable sites of these proteases indicated that the former and latter are the peptides Asp41–Lys75 (3.8 kDa) and Asp41–Arg63 (2.5 kDa), respectively. All together, the cross-linked site of [¹²⁵I]AzQ should be within the sequence region Asp41–Arg63 (Figure 7B).

Unfortunately, we could not identify the cross-linked region in the ND1 subunit because of its remarkably hydrophobic nature and the low yield of the cross-linking reaction.

DISCUSSION

Our knowledge about the mechanism of complex I including the action manner of numerous specific inhibitors is still largely limited. Detailed studies on the action manner of the inhibitors are necessary to obtain further insights into the function of the membrane domain of the enzyme (49). In the present study, the synthesis of [¹²⁵I]AzQ allowed us to identify the binding site of a core structure of quinazoline-type inhibitors with a photoaffinity labeling technique. Specific cross-linking with complex I was detected in the 49 kDa and ND1 subunits with a frequency of ~4:1. We recently demonstrated that photoreactive acetogenin and piperazine-type inhibitor specifically binds to the ND1 and 49 kDa subunits, respectively (23, 49). Concerning acetogenin, a photoreactive phenyldiazirine group was attached to one of the two toxophoric core structures. Further, a number of studies indicated the functional importance of the two subunits for the enzyme activity (5, 7, 17–19, 31). Taken together, the 49 kDa and ND1 subunits must be key components connecting the redox reaction in the peripheral arm and the proton pumping event in the membrane arm. The earlier photoaffinity labeling studies indicated that pyridaben (21) and fenpyroximate (22) derivatives bind to the PSST and the ND5 subunits of bovine complex I, respectively. It should however be realized that as a photoreactive phenyldiazirine group of the two derivatives was attached to the “side chain” moiety which is far from the toxophoric heterocyclic rings, one cannot exclude the possibility that the positions of the heterocyclic rings at bound state in the enzyme are not necessarily on the PSST and ND5 subunits.

It is worth discussing the implications of the finding that [¹²⁵I]AzQ cross-linked to two different subunits at the same time. In this context, Casida and colleagues (53) showed that a photoreactive agonist [³H]azidoepibatidine ([³H]AzEPI) of the homopentameric mollusk acetylcholine binding protein (AChBP) cross-links to either Tyr195 of loop C or Met116

of loop E at a similar frequency. Considering that the calculated bond angle of $-\text{N}=\text{N}^+=\text{N}^-$ for phenylazido is 165°, not 180°, and hence there are two azido conformers with similar energy levels, they interpreted the result to mean that the azido group of [³H]AzEPI is positioned between Tyr195 and Met116 which exist close to each other, and one conformer reacts to Tyr195 and the other to Met116. The docking model of AzEPI into AChBP supported this scenario.

Thus, the fact that an azido group takes two stable conformations against the benzene ring plane is important to elucidate the manner of the cross-linking of this photolabile group. Although the crystal structure of the membrane domain of complex I is not available at present, our results strongly suggest that the 49 kDa and ND1 subunits are in contact with each other and that the azido group of [¹²⁵I]AzQ is located between them. The sequence region Asp41–Arg63 (23 amino acids) in the 49 kDa subunit is a possible area of contact with the ND1 subunit. This notion is consistent with a 3D model of *E. coli* complex I proposed by Sazanov and colleagues (29). That is, they arranged the NuoH (ND1) and NuoD (49 kDa) subunits adjacent to each other in the interfacial region of the peripheral and membrane arms. Schuler et al. reported that a photoreactive pyridaben analogue binds to the PSST, which is a neighbor of the 49 kDa subunit (3) and ND1 subunits at low (<20 nM) and high (~50–250 nM) concentrations, respectively (21). However, they concluded that the binding to the ND1 subunit is not associated with the inhibition of the enzyme’s activity; i.e., it is nonspecific. Although we here hypothesized that the photo-cross-linking of the two subunits is due to two conformers of the azido group, we cannot exclude the possibility that complex I in situ has two or more conformers.

On the basis of an amino acid sequence alignment of the 49 kDa subunit from various organisms, we will next consider the functionality of the labeled region (i.e., Asp41–Arg63). In the crystal structure of the Nqo4 subunit (49 kDa) in *T. thermophilus* (3), some N-terminal residues corresponding to this region were not observed due to a lack of electron density and so were not modeled (Figure 8). Nevertheless, taking into consideration the overall architecture of the hydrophilic domain of complex I in *T. thermophilus*, this region must be located in the membrane domain and probably comprises the quinone/inhibitor binding pocket, as illustrated in Figure 8A,B (3, 29). It may be noted that the position of the 49 kDa subunit in this model is fairly different from that proposed for *Y. lipolytica* complex I based on antibody labeling study (54). On the other hand, from the mutagenesis studies of *Y. lipolytica*, Brandt and colleagues concluded that a broad cavity formed by the PSST and 49 kDa subunits comprises the active site for ubiquinone reduction and the binding domain for traditional inhibitors (19). They showed that His95, Leu98, and Arg99 in the *Y. lipolytica* 49 kDa subunit are critical for the quinone reduction activity (19). These residues are actually located within the area corresponding to the labeled region found in the present study (Figure 8C). In contrast, the mutagenesis of strictly conserved residues (E211, E218, R224, and L225) far from the labeled region had virtually no effect on sensitivity to the quinazoline-type inhibitor DQA or the enzyme activity (19).

In conclusion, we carried out a photoaffinity labeling study using a newly synthesized [¹²⁵I]AzQ which has a photore-

active group in the core scaffold. [¹²⁵I]AzQ specifically binds to the 49 kDa and ND1 subunits with a frequency of about ~4:1. A combination of different proteolyzes of the cross-linked 49 kDa subunit revealed the binding site of the core scaffold of [¹²⁵I]AzQ to be located within the sequence Asp41–Arg63, which may be located in the membrane arm and also critical for the quinone binding.

ACKNOWLEDGMENT

We thank Prof. Yasuo Shinohara (University of Tokushima, Japan) for advice on the assay of ADP/ATP carrier and Dr. Takahisa Kato (Radioisotope Research Center of Kyoto University) for excellent technical assistance.

SUPPORTING INFORMATION AVAILABLE

Synthesis of [¹²⁵I]AzQ, Table S1, and Figures S1–S5. This material is available free of charge via the Internet at <http://pubs.acs.org>.

REFERENCES

- Walker, J. E. (1992) The NADH-ubiquinone oxidoreductase (complex I) of respiratory chains. *Q. Rev. Biophys.* 25, 253–324.
- Carroll, J., Fearnley, I. M., Skehel, J. M., Shannon, R. J., Hirst, J., and Walker, J. E. (2006) Bovine complex I is a complex of 45 different subunits. *J. Biol. Chem.* 281, 32724–32727.
- Sazanov, L. A., and Hinchliffe, P. (2006) Structure of the hydrophilic domain of respiratory complex I from *Thermus thermophilus*. *Science* 311, 1430–1436.
- Ohnishi, T. (1998) Iron-sulfur clusters/semiquinones in complex I. *Biochim. Biophys. Acta* 1364, 186–206.
- Yagi, T., and Matsuno-Yagi, A. (2003) The proton-translocating NADH-quinone oxidoreductase in the respiratory chain: the secret unlocked. *Biochemistry* 42, 2266–2274.
- Hirst, J. (2005) Energy transduction by respiratory complex I; an evaluation of current knowledge. *Biochem. Soc. Trans.* 33, 525–529.
- Brandt, U. (2006) Energy converting NADH:quinone oxidoreductase (complex I). *Annu. Rev. Biochem.* 75, 69–92.
- Friedrich, T., Van Heek, P., Leif, H., Ohnishi, T., Forche, E., Kunze, B., Jansen, R., Trowitzsch-Kienast, W., Höfle, G., Reichenbach, H., and Weiss, H. (1994) Two binding sites of inhibitors in NADH:ubiquinone oxidoreductase (complex I). *Eur. J. Biochem.* 219, 691–698.
- Degli Esposti, M. (1998) Inhibitors of NADH-ubiquinone reductase: an overview. *Biochim. Biophys. Acta* 1364, 222–235.
- Miyoshi, H. (1998) Structure-activity relationships of some complex I inhibitors. *Biochim. Biophys. Acta* 1364, 236–244.
- Magnitsky, S., Touloukhonova, L., Yano, T., Sled, V. D., Hägerhäll, C., Grivennikova, V. G., Burbaev, D. S., Vinogradov, A. D., and Ohnishi, T. (2002) EPR characterization of ubisemiquinones and iron-sulfur cluster N2, central components of the energy coupling in the NADH-ubiquinone oxidoreductase (complex I) in situ. *J. Bioenerg. Biomembr.* 34, 193–208.
- Heinrich, H., and Werner, S. (1992) Identification of the ubiquinone-binding site of NADH-ubiquinone oxidoreductase (complex I) from *Neurospora crassa*. *Biochemistry* 31, 11413–11419.
- Gong, X., Xie, T., Yu, L., Hesterberg, M., Scheide, D., Friedrich, T., and Yu, C.-A. (2003) The ubiquinone-binding site in NADH-ubiquinone oxidoreductase from *Escherichia coli*. *J. Biol. Chem.* 278, 25731–25737.
- Okun, J. G., Lümmen, P., and Brandt, U. (1999) Three classes of inhibitor share a common binding domain in mitochondrial complex I (NADH-ubiquinone oxidoreductase). *J. Biol. Chem.* 274, 2625–2630.
- Ino, T., Nishioka, T., and Miyoshi, H. (2003) Characterization of inhibitor binding sites of mitochondrial complex I using fluorescent inhibitor. *Biochim. Biophys. Acta* 1605, 15–20.
- Ahlers, P. M., Zwicker, K., Kerscher, S., and Brandt, U. (2000) Function of conserved acidic residues in the PSST homologue of complex I (NADH-ubiquinone oxidoreductase) from *Yarrowia lipolytica*. *J. Biol. Chem.* 275, 23577–23582.
- Kashani-Poor, N., Zwicker, K., Kerscher, S., and Brandt, U. (2001) A central functional role for the 49-kDa subunit within the catalytic core of mitochondrial complex I. *J. Biol. Chem.* 276, 24082–24087.
- Prieur, I., Lunardi, J., and Dupuis, A. (2001) Evidence for a quinone binding site close to the interface between NuoD and NuoB subunits of complex I. *Biochim. Biophys. Acta* 1504, 173–178.
- Tocilescu, M. A., Fendel, U., Zwicker, K., Kerscher, S., and Brandt, U. (2007) Exploring the ubiquinone binding cavity of respiratory complex I. *J. Biol. Chem.* 282, 29514–29520.
- Earley, F. G. P., Patel, S. D., Ragan, C. I., and Attardi, G. (1987) Photolabeling of a mitochondrially encoded subunit of NADH dehydrogenase with [³H]dihydrorotenone. *FEBS Lett.* 219, 108–113.
- Schuler, F., Yano, T., Bernardo, S. D., Yagi, T., Yankovskaya, V., Singer, T. P., and Casida, J. E. (1999) NADH-quinone oxidoreductase: PSST subunit couples electron transfer from iron-sulfur cluster N2 to quinone. *Proc. Natl. Acad. Sci. U.S.A.* 96, 4149–4153.
- Nakamaru-Ogiso, E., Sakamoto, K., Matsuno-Yagi, A., Miyoshi, H., and Yagi, T. (2003) The ND5 subunit was labeled by a photoaffinity analogue of fenyproximate in bovine mitochondrial complex I. *Biochemistry* 42, 746–754.
- Murai, M., Ishihara, A., Nishioka, T., Yagi, T., and Miyoshi, H. (2007) The ND1 subunit constructs the inhibitor binding domain in bovine heart mitochondrial complex I. *Biochemistry* 46, 6409–6416.
- Ichimaru, N., Murai, M., Abe, M., Hamada, T., Yamada, Y., Makino, S., Nishioka, T., Makabe, H., Makino, A., Kobayashi, T., and Miyoshi, H. (2005) Synthesis and inhibition mechanism of Δlac-acetogenins: a novel type of inhibitor of bovine heart mitochondrial complex I. *Biochemistry* 44, 816–825.
- Murai, M., Ichimaru, N., Abe, M., Nishioka, T., and Miyoshi, H. (2006) Mode of inhibitory action of Δlac-acetogenins, a new class of inhibitors of bovine heart mitochondrial complex I. *Biochemistry* 45, 9778–9787.
- Brunner, J. (1993) New photolabeling and crosslinking methods. *Annu. Rev. Biochem.* 62, 483–514.
- Dormán, G., and Prestwich, G. D. (2000) Using photolabile ligands in drug discovery and development. *Trends Biotechnol.* 18, 64–76.
- Holt, P. J., Morgan, D. J., and Sazanov, L. A. (2003) The location of NuoL and NuoM subunits in the membrane domain of the *Escherichia coli* complex I. *J. Biol. Chem.* 278, 43114–43120.
- Baranova, E. A., Holt, P. J., and Sazanov, L. A. (2007) Projection structure of the membrane domain of *Escherichia coli* respiratory complex I at 8 angstrom resolution. *J. Mol. Biol.* 366, 140–154.
- Zhang, H., Lerro, K. A., Yamamoto, T., Lien, T. H., Sastry, L., Gwinowicz, M. A., and Nakanishi, K. (1994) The location of the chromophore in rhodopsin: a photoaffinity study. *J. Am. Chem. Soc.* 116, 10165–10173.
- Yagi, T., and Hatefi, Y. (1988) Identification of the dicyclohexylcarbodiimide-binding subunit of NADH-ubiquinone oxidoreductase (complex I). *J. Biol. Chem.* 263, 16150–16155.
- Kao, M. C., Matsuno-Yagi, A., and Yagi, T. (2004) Subunit proximity in the H⁺-translocating NADH-quinone oxidoreductase probed by zero-length cross-linking. *Biochemistry* 43, 3750–3755.
- Yamashita, T., Ino, T., Miyoshi, H., Sakamoto, K., Osanai, A., Nakamaru-Ogiso, E., and Kita, K. (2004) Rhodoquinone reaction site of mitochondrial complex I in parasitic helminth *Ascaris suum*. *Biochim. Biophys. Acta* 1608, 97–103.
- Smith, A. L. (1967) Preparation, properties and conditions for assay of mitochondria: slaughterhouse material, small scale. *Methods Enzymol.* 10, 81–86.
- Matsuno-Yagi, A., and Hatefi, Y. (1985) Studies on the mechanism of oxidative phosphorylation. *J. Biol. Chem.* 260, 14424–14427.
- Majima, E., Koike, H., Hong, Y.-M., Shinohara, Y., and Terada, H. (1993) Characterization of cysteine residues of mitochondrial ADP/ATP carrier with the SH-reagents eosin 5-maleimide and N-ethylmaleimide. *J. Biol. Chem.* 268, 22181–22187.
- McIntyre, J. O., Latruffe, N., Brenner, S. C., and Fleischer, S. (1988) Comparison of 3-hydroxybutyrate dehydrogenase from bovine heart and rat liver mitochondria. *Arch. Biochem. Biophys.* 262, 85–98.
- Laemmli, U. K. (1970) Cleavage of structural proteins during the assembly of the head of bacteriophage T4. *Nature* 227, 680–685.
- Zerbetto, E., Vergani, L., and Dabbeni-Sara, F. (1997) Quantification of muscle mitochondrial oxidative phosphorylation enzymes via histochemical staining of blue native polyacrylamide gels. *Electrophoresis* 18, 2059–2064.

40. Schägger, H. (1995) Native electrophoresis for isolation of mitochondrial oxidative phosphorylation protein complexes. *Methods Enzymol.* 260, 190–202.
41. Sazanov, L. A., Peak-Chew, S. Y., Fearnley, I. M., and Walker, J. E. (2000) Resolution of the membrane domain of bovine complex I into subcomplexes: Implications for structural organization of the enzyme. *Biochemistry* 39, 7229–7235.
42. Cleveland, D. W., Fishcher, M. W., Kirschner, M. W., and Laemmli, U. K. (1977) Peptide mapping by limited proteolysis in sodium dodecyl sulfate and analysis by gel electrophoresis. *J. Biol. Chem.* 252, 1102–1106.
43. Omori, A., Ichinose, S., Kitajima, S., Shimotohno, K. W., Murashima, Y. L., Shimotohno, K., and Seto-Ohshima, A. (2002) Gerbils of a seizure-sensitive strain have a mitochondrial inner membrane protein with different isoelectric points from those of a seizure-resistant strain. *Electrophoresis* 23, 4167–4174.
44. Schägger, H. (2006) Tricine-SDS-PAGE. *Nat. Protoc.* 1, 16–21.
45. Schägger, H., and von Jagow, G. (1991) Blue native electrophoresis for isolation of membrane protein complexes in enzymatically active form. *Anal. Biochem.* 199, 223–231.
46. Wittig, I., Braun, H. P., and Schägger, H. (2006) Blue native PAGE. *Nat. Protoc.* 1, 418–428.
47. Carroll, J., Fearnley, I. M., and Walker, J. E. (2006) Definition of the mitochondrial proteome by measurement of molecular masses of membrane proteins. *Proc. Natl. Acad. Sci. U.S.A.* 103, 16170–16175.
48. Carroll, J., Fearnley, I. E., Shannon, R. J., Hirst, J., and Walker, J. E. (2003) Analysis of the subunit composition of complex I from bovine heart mitochondria. *Mol. Cell. Proteomics* 2, 117–126.
49. Ichimaru, N., Murai, M., Kakutani, N., Kako, J., Ishihara, A., Nakagawa, Y., Nishioka, T., Yagi, T., and Miyoshi, H. (2008) Synthesis and characterization of new piperazine-type inhibitors for mitochondrial NADH-ubiquinone oxidoreductase (complex I). *Biochemistry* 47, 10816–10826.
50. Sakamoto, K., Miyoshi, H., Ohshima, M., Kuwabara, K., Kano, K., Akagi, T., Mogi, T., and Iwamura, H. (1998) Role of isoprenyl tail of ubiquinone in reaction with respiratory enzymes: studies with bovine heart mitochondrial complex I and *Escherichia coli* bo-type ubiquinol oxidase. *Biochemistry* 37, 15106–15113.
51. Matsumoto, Y., Murai, M., Fujita, D., Sakamoto, K., Miyoshi, H., Yoshida, M., and Mogi, T. (2006) Mass spectrometric analysis of the ubiquinol-binding site in cytochrome bd from *Escherichia coli*. *J. Biol. Chem.* 281, 1905–1912.
52. Fendel, U., Tocilescu, M. A., Kerscher, S., and Brandt, U. (2008) Exploring the inhibitor binding pocket of respiratory complex I. *Biochim. Biophys. Acta* 1777, 660–665.
53. Tomizawa, M., Maltby, D., Medzihradzky, K. F., Zhang, N., Durkin, K. A., Presley, J., Talley, T. T., Taylor, P., Burlingame, A. L., and Casida, J. E. (2007) Defining nicotinic agonist binding surfaces through photoaffinity labeling. *Biochemistry* 46, 8798–8806.
54. Zickermann, V., Bostina, M., Hunte, C., Ruiz, T., Radermacher, M., and Brandt, U. (2003) Functional implication from an unexpected position of the 49-kDa subunit of NADH-ubiquinone oxidoreductase. *J. Biol. Chem.* 278, 29072–29078.

BI8019977